Simultaneous waveform inversion of seismic-while-drilling data for P-wave velocity, density and source parameters

Jinji Li, Scott Keating, Nasser Kazemi, Roman Shor, and Kristopher A. Innanen*

Summary

Full waveform inversion (FWI), as an optimization-based approach in estimating subsurface models, is limited by incomplete acquisition and illumination of the subsurface. Adding data corresponding to new and independent ray paths as input could lead to significant increases in the reliability of FWI models. In principle, seismic-while-drilling (SWD) technology can supply these additional ray paths, however, it introduces a new suite of unknowns, namely precise source locations (i.e., drilling path), source signature, and radiation characteristics. Here we formulate a new elastic FWI algorithm in which source positions and radiation patterns join the velocity and density values of the grid cells as unknowns to be determined. We then carry out a numerical inversion experiment with the SWD sources located along a plausible well-trajectory through a synthetic model. These SWD sources are supplemented by explosive sources and multicomponent receivers at the surface, simulating a conventional acquisition geometry. The subsurface model and SWD source properties are recovered and analyzed. After adding SWD data, both the inversion of elastic properties and source mechanisms get considerably enhanced, and the inversion shows a directional preference on the well trajectories. The analysis suggests that, in principle, SWD participation improves the accuracy of FWI models. However, further related study is required to provide more comprehensive radiation patterns of the SWD sources.

Introduction

Full waveform inversion (FWI) is a procedure for using seismic data to estimate the physical properties of the Earth. By iteratively minimizing a misfit function representing the distance in the data space between synthetically modeled and experimentally recorded data, the subsurface models of physical parameters and other relevant unknowns can be updated to produce high-resolution model estimates (Tarantola, 1984; Pan et al., 2015). This technique is recognized as promising in both academic and industrial applications. However, when applying FWI to field data, practical issues can strongly affect the accuracy of the inverted models. One key factor affecting inversion results is limited geometric coverage in seismic data acquisition. FWI is nonlinear and ill-posed, so dense acquisition is essential (Kazemi et al., 2018). In surface field data, ray paths interacting with the unknown medium with transmission-like geometries are largely limited to diving waves, necessitating long-offset acquisition. Transmission ray paths (which are more readily available in cross-well and VSP experiments), if available are major contributors to the construction of low-wavenumber components of an FWI model. Seismic rays tend to bend toward high-velocity zones such as salt bodies and move away from low-velocity zones such as overpressure regions. The non-uniform ray path coverage introduces shadow zones. The shadow zones are in the null space of the FWI inversion operator. Thus, the physical properties in those regions cannot be recovered unless we add a priori knowledge about the subsurface to fill in the gaps in ray path coverage. The alternative is to introduce subsurface sources with unique ray paths compared to surface seismic acquisition to improve the ray path coverage of the subsurface. In principle, adding new, independent, and especially transmission-like ray paths to the seismic data used in FWI can lead to significant improvements in inversion accuracy.

Drill-bit-rock interactions can generate elastic waves from source locations along a well path and be recorded by surface receivers, suggesting that the SWD datasets can contribute to FWI. The drilling program may be significantly influenced by uncertainties in formation tops and heterogeneities in complex stratigraphy. Avoiding high pore pressure zones and near-real-time updates of the drilling parameters require knowledge of the seismic velocity of formation interacting with the drill bit (Auriol et al., 2021). SWD technology may improve the prediction of upcoming formation changes as accuracy is higher with a shorter ray path. The drilling program can be de-risked by using reflection information via multi-offset processing to predict overpressure zones or key objectives (Cornish et al., 2007). In recent years, the potential of SWD in seismic imaging and inversion has attracted renewed attention (Kazemi et al., 2014; Poletto et al., 2020; Nejadi et al., 2020). Kazemi (2020) implemented a two-stage sequential SWD-FWI in which inversion with only SWD sources was followed by inversion with the conventional acquisition, producing evidence of SWD datasets' positive impact on FWI. However, a complete feasibility study incorporating several additional practical constraints is needed. First, the directionality features of drill bit radiation patterns need to be accounted for. Borehole inclination and azimuth change the vertical and horizontal components of the SWD signal. Second, the complicated character of the continuously-radiating source drill-bit is difficult to plausibly model in FWI with a static, known, and simply-radiating point source, so some accommodation for the complex sources needs to be made. Third, the drill radiation contains rich P- and S-wave signals, which cannot be taken advantage of within acoustic models. Motivated by this, we adapt the frequency domain multi-parameter elastic FWI scheme of Keating and Innanen (2020), in which source radiation patterns join the velocity and density values of the grid cells as unknowns to be determined, to the problem of SWD-FWI as driven by surface acquisition geometries with known explosive sources.

Theory

In the frequency domain, for a given frequency, the optimization problem in the form of L2 norm is as follow:

$$\boldsymbol{argmin}_x \phi(\boldsymbol{x}) = \frac{1}{2}\|\boldsymbol{Ru} - \boldsymbol{d}\|_2^2, \qquad s.t.\ \boldsymbol{Su} = \boldsymbol{f}, \tag{1}$$

where $\boldsymbol{x}$ is a set of inversion variables combining the subsurface and source models. $\boldsymbol{R}$ is the sampling matrix representing the measurements of receivers, $\boldsymbol{u}$ stands for the wavefield from a source position to an arbitrary receiver, $\boldsymbol{d}$ is the observed data between a source-receiver pair, $\boldsymbol{S}$ is the finite-difference modeling operator, and $\boldsymbol{f}$ is the source term. Here $\phi(\boldsymbol{x})$ includes the summation over frequencies, but we do not state it here for convenience. We use the adjoint state method to determine our objective function's first and second-order partial derivatives (Plessix, 2006). For one source-receiver pair, The Lagrangian of the problem is:

$$L(\boldsymbol{x}) = \frac{1}{2}\|\boldsymbol{R\bar{u}} - \boldsymbol{d}\|_2^2 + (\boldsymbol{S\bar{u}} - \boldsymbol{f}, \lambda), \tag{2}$$

where $\bar{\boldsymbol{u}}$ denotes the solution of the forward problem, and λ is a Lagrange multiplier. Using the adjoint state method, the gradient of our objective function with respect to inversion variables can be written as:

$$\frac{d\phi}{d\boldsymbol{x}} = \frac{\partial L(\bar{\boldsymbol{u}}, \bar{\lambda})}{\partial \boldsymbol{x}}, \tag{3}$$

where $\bar{\lambda}$ is the adjoint wavefield acquired through a forward propagation with data residual as the source term:

$$S^{\dagger}\bar{\lambda} = R^T(\boldsymbol{d} - \boldsymbol{R\bar{u}}). \tag{4}$$

The gradient for the non-source models and source terms are shown by:

$$\boldsymbol{g}(\boldsymbol{m}) = (\frac{\partial}{\partial \boldsymbol{m}}\boldsymbol{S\bar{u}}, \bar{\lambda}), \tag{5}$$

$$\frac{d\phi}{d\boldsymbol{f}} = \sum_n (-\Re(\bar{\lambda}_n) + i\Im(\bar{\lambda}_n)), \tag{6}$$

where n is the number of SWD sources. Each inversion variable has a number of elements equal to the number of points in the wavefield grid used in forward modeling multiplied by the number of the SWD sources considered. Such large dimensionality makes it necessary to have more restrictions to source-related variables. Consider a variable $\boldsymbol{f}_k$ that controls the moment tensors of a point source. The derivative of the objective function with respect to such a variable is an extension of the derivative with respect to the force term:

$$\frac{d\phi}{d\boldsymbol{f}_k} = \sum_n (-\Re(\bar{\lambda}_n)\frac{d\boldsymbol{f}_{R_n}}{d\boldsymbol{f}_k} + \Im(\bar{\lambda}_n)\frac{d\boldsymbol{f}_{I_n}}{d\boldsymbol{f}_k}), \tag{7}$$

where the first part within the summation on the right-hand side is the derivative of the real component of the source term w.r.t. $\boldsymbol{f}_k$, and the second part is the derivative of the imaginary component of the source term w.r.t. $\boldsymbol{f}_k$.

The variables in this simultaneous inversion represent the whole elastic model and the drilling sources. The corresponding gradients in Equations (5) and (6) are contributed to from different datasets: the gradient $\boldsymbol{g}(\boldsymbol{m})$ for subsurface parameters benefits from all the wavefields generated by surface explosive and independent SWD sources in our inversion, whereas the SWD source inversion only relies on the data generated by drilling sources.

We use the anelastic finite-difference approach to solve the 2-D viscoelastic wave equations in the frequency domain (Pratt, 1990), and 2-D moment tensor matrices to represent the source terms. Isotropic moment tensors are used for the surface sources, and general tensors are assumed for the SWD sources. Technically, the main issue in formulating a stable source-model simultaneous inversion is in the discrete representation of the seismic sources. For a point source, the m, n elements in the moment tensor matrix denote the derivative of the displacement in the m direction with respect to the n direction, so it is necessary to use derivatives within a small region in the finite-difference model accurately (Keating and Innanen, 2020). Figure 1 illustrates our first-order difference approach in treating the source-related derivatives. For a point source located midway between two finite-difference cell centers in Figure 1 (a), the approximation of $M_{11} = 1$ in the horizontal direction can be represented by the two adjacent cells as $-\frac{1}{\Delta x}$ and $\frac{1}{\Delta x}$, respectively. If the source position is not equidistant between finite-difference cell centers, we use three continuous weighted members to approximate the first-order spatial derivatives. The finite-difference weights used for a source location between two finite-difference grid lines will be a weighted average of the importance used for a source at either of the bounding grid lines, as shown in figure 1 (b). Extending this concept to two dimensions, the 2-D sources are maximally defined by the weighting between intersections of nine grid cells in a small surrounding region if the moment tensors in both directions are considered. This treatment makes it possible to represent a point source in arbitrary locations.

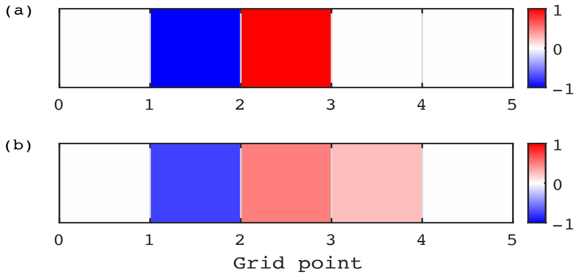

Figure 1: Scaled weights for approximating a derivative in one dimension. (a) weights for source location $x = 2$. (b) weights for source location $x = 2.25$.

Examples

The numerical tests in this section are based on synthetic models to evaluate the performance and investigate the potential of combining seismic-while-drilling datasets with simultaneous model-source full waveform inversion. The true models are shown in Figure 2. The horizontal size of the model is considerably larger than the target inversion zone, because in practice the drilling sites are often far from surface sensors. Our inversion target is roughly half the height of the larger model, as indicated by the dashed rectangle. Two acquisition geometries are considered here: one with a vertical drilling path and the other with a deviated drilling path.

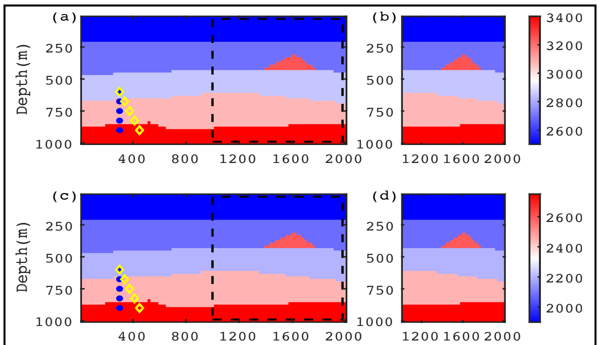

Figure 2: True subsurface properties of the synthetic model and the positions for SWD sources. (a) Whole velocity model with a vertical and a deviated drilling trajectory. (b) Target velocity model. (c) Whole density model with a vertical and a deviated drilling trajectory. (d) Target density model.

Both geometries include explosive sources and multicomponent receivers at the surface (24 explosive sources and 48 receivers are set on the surface of the inversion target, acting as a conventional surface acquisition). The receivers near the surface have a 700-meter offset from the well location. Drilling trajectories are added in the deeper section of the left-hand side of the model with twenty independent sources represented by random moment tensors in a range of 0 to 1. We assume that (1) the drill can be treated as if it occupies a discrete sequence of quasi-static positions along the drill trajectory, and (2) the SWD data can be analyzed into the discrete FWI frequencies we select below; the problem of transformation of SWD signals into useable seismic data has been discussed by Kazemi et al (2020). The drill sources are located between 600m-900m depth, and the deviated drilling trajectory is in the horizontal range of 300m to 500m.

A multi-scale approach is used for our inversion. We consider 20 total frequency bands, each containing 6 sub-frequencies. The starting frequencies of every band are set to 1 Hz, while the ending frequencies linearly increase from 2 Hz (for the first band) to 15 Hz (at the last).

We carry out the inversion for surface only, surface and vertical well, and surface and deviated well cases. One of the major advantages of our inversion is the intervention of additional sources can provide feasible information of the subsurface anelastic models, so the starting model for our inversion is based on the assumption that there is little prior information available. The initial anelastic properties are constant in each parameter, being the background values of the true models. The moment tensors start with random values from 0 to 1.

The inversion results of subsurface properties are shown in Figure 3. Figure 3 (a) shows a crude estimate of the P-wave velocity with the surface-only acquisition. The region below the high-velocity triangle is in the shadow zone of the surface acquisition and is not well recovered, as evidenced by indistinct structures in the density model in Figure 3 (b). However, the inversion gets better when including the SWD data. Figures 3 (c) and (d) are the inversion results with a vertical drilling path. This acquisition provides a more reliable model estimation, shown by a better recovery in the left part of the V_P model, and an improved ρ image. We acquire the best inversion when a deviated drilling trajectory is considered, as is shown in Figure 3 (e) and (f). In this case, energy coverage is improved within the velocity model except in the lower-right regions, where negligible additional ray paths are provided by the SWD acquisition. The density model and layer structure are also better resolved in this case.

Figure 4 shows the estimation of moment tensors by cross plots. The x-axis denotes the true value, while the y-axis is the estimated value. The moment tensors along a vertical drilling path, which are shown by Figure 4 (a), (c), and (e), show a systematic error because of a shortage of measured horizontal components. However, as shown in Figure 4 (b), (d), and (f), the estimation is enhanced considerably with a deviated drilling trajectory. In vertical drilling, P radiations are stronger along the vertical direction. In other words, the horizontal component is weak in the SWD data for vertical drilling with surface geophones. However, in deviated wells, both vertical and horizontal components are present. Thus, both the inversion of surface and deviated drilling data result in superior performance.

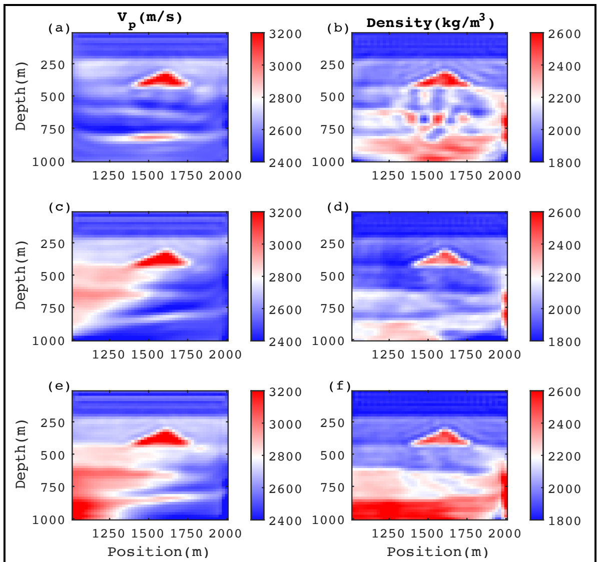

Figure 3: Inversion of subsurface properties. (a)-(b), inversion of V_P and ρ with surface acquisition. (c)-(d), inversion of V_P and ρ with surface acquisition and a vertical well. (e)-(f), inversion of V_P and ρ with surface acquisition and a deviated well.

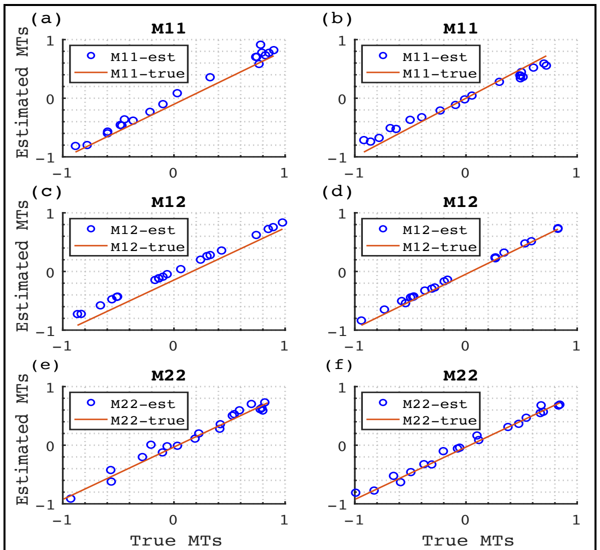

Figure 4: Estimation of moment tensors of the SWD sources. (a), (c), and (e), cross plots of true and estimated moment tensors along a vertical drilling trajectory. (b), (d), and (f), cross plots of true and estimated moment tensors along a deviated drilling trajectory.

Discussion

The numerical examples show that a source-model simultaneous inversion is feasible in a surface + SWD setting, and the simulations allow the impact of the additional ray paths to be understood and analyzed. We believe in this formulation that the key elements needed to explain the SWD signature and begin to use it, are in place. This study also suggests some important directions for further study. First, although we have not allowed it to be a free unknown as yet, this framework has the capacity to estimate source positions as well as radiation patterns, thus in principle allowing SWD-FWI technology to help refine drill position estimates. Such inversion has the potential to help the ahead-of-the-bit estimation in SWD, though computational speed and expense would need to be reduced for this to be practically realized. Our multi-band inversion currently uses random moment tensors with impulsive energy in each frequency. However, it is possible to design a more realistic representation considering both the drill-bit-rock mechanism with moment tensors and frequency dependence.

Conclusions

This work explores the potential of taking advantage of the seismic-while-drilling data to compensate for the incomplete surface acquisition in simultaneous full waveform inversion. Numerical examples demonstrate that the additional ray paths provided in an SWD dataset help to provide a better FWI result. The inclusion of SWD data improves the inversion of elastic properties; we also found that the moment tensor inversion had higher reliability when a deviated drilling path was considered because more feasible components are recorded on the surface. This leads us to conclude that seismic-while-drilling data offers the potential to improve inversion results. Further research is still required to provide more comprehensive conclusions, especially with respect to a more accurate moment tensor representation of the drill-bit rock interactions mechanisms and an advanced inversion strategy that will fit a more practical case. Additionally, the source signature of various types of drill bits should be quantified to detail the P and S-wave components.

Acknowledgements

We thank the sponsors of CREWES for continued support. This work was funded by CREWES industrial sponsors and NSERC (Natural Science and Engineering Research Council of Canada) through the grant CRDPJ 543578-19.